Measurements of the Anisotropic In-Plane Resistivity of Underdoped FeAs-Based Pnictide Superconductors

J. J. Ying,[1] X. F. Wang,[1] T. Wu,[1] Z. J. Xiang,[1] R. H. Liu,[1] Y. J. Yan,[1] A. F. Wang,[1] M. Zhang,[1] G. J. Ye,[1] P. Cheng,[1] J. P. Hu,[2] and X. H. Chen[1,*]

[1]*Hefei National Laboratory for Physical Science at Microscale and Department of Physics, University of Science and Technology of China, Hefei, Anhui 230026, People's Republic of China*

[2]*Department of Physics, Purdue University, West Lafayette, Indiana 47907, USA*

(Received 13 December 2010; published 2 August 2011)

We systematically investigated the in-plane resistivity anisotropy of electron-underdoped $EuFe_{2-x}Co_xAs_2$ and $BaFe_{2-x}Co_xAs_2$ and hole-underdoped $Ba_{1-x}K_xFe_2As_2$. Large in-plane resistivity anisotropy was found in the former samples, while *tiny* in-plane resistivity anisotropy was detected in the latter ones. When it is detected, the anisotropy starts above the structural transition temperature and increases smoothly through it. As the temperature is lowered further, the anisotropy takes a dramatic enhancement through the magnetic transition temperature. We found that the anisotropy is universally tied to the presence of T-linear behavior of resistivity. Our results demonstrate that the nematic state is caused by electronic degrees of freedom, and the microscopic orbital involvement in the magnetically ordered state must be fundamentally different between the hole- and electron-doped materials.

DOI: 10.1103/PhysRevLett.107.067001 PACS numbers: 74.25.F−, 74.70.Xa

The newly discovered iron-based high temperature superconductors provide a new family of materials to explore the mechanism of high-T_c superconductivity besides high-T_c cuprate superconductors [1–4]. The undoped nonsuperconducting ''parent'' compounds of LFeAsO (L denotes the rare-earth-metal elements, and this compound is abbreviated as 1111) and AFe_2As_2 (A denotes the alkali-earth-metal elements, and this compound is abbreviated 122) undergo a tetragonal to orthorhombic structure transition and a spin density wave (SDW) transition. The structure transition temperature (T_S) is higher than the SDW transition temperature (T_N) in the 1111 system, while for the 122 parent compound T_N is almost the same as T_S. Superconductivity arises when both transitions are suppressed via electron or hole doping. The origin of the structure transition and SDW transition is still unclear; it was proposed that antiferromagnetic fluctuation [5,6] or orbital ordering [7–9] may play an important role in driving the transitions.

Recent works showed a large in-plane resistivity anisotropy below T_S or T_N in the Co-doped Ba122 system, though the distortion of the orthorhombic structure is less than 1% [10,11] in the SDW state. The resistivity is smaller along the antiferromagnetic a direction than along the ferromagnetic b direction, which is opposite of our intuitive thinking that scattering from spin fluctuations would ordinarily result in a higher resistivity along the antiferromagnetic a direction [10]. Moreover, the resistivity anisotropy grows with doping and approaches its maximum close to the point where superconductivity emerges. Other experiments also reported the existence of anisotropy in many different physical properties in the SDW state of iron pnictides including magnetic exchange coupling [12], Fermi surface topology [13], and local density distribution [14]. Electronic anisotropies have also been observed in many other materials, including underdoped cuprates, quantum Hall systems, and $Sr_3Ru_2O_7$ [15,16]. In cuprates, electronic anisotropy cannot be explained by small structural orthorhombicity [17,18], and it has been proposed the large electron anisotropy is due to the emergence of an electron nematic phase which exhibits quasi-one-dimensional (1D) liquid-crystal-like electronic structures. This idea has been widely investigated in the other two systems as well. In iron pnictides, the origin of the electronic anisotropy is still elusive because of their complicated electronic structures and the presence of many different degrees of freedom.

In this Letter, we systematically investigated the in-plane resistivity anisotropy of electron-underdoped $EuFe_{2-x}Co_xAs_2$ and $BaFe_{2-x}Co_xAs_2$ and hole-underdoped $Ba_{1-x}K_xFe_2As_2$ systems. Large in-plane resistivity anisotropy behavior was found below T_S or T_N in $EuFe_{2-x}Co_xAs_2$ and $BaFe_{2-x}Co_xAs_2$, while in-plane anisotropy is dramatically decreased and barely observable in $Ba_{1-x}K_xFe_2As_2$. The resistivity shows T-linear behavior above the temperature wherever the resistivity anisotropy starts to emerge. In the $Ba_{1-x}K_xFe_2As_2$, no T-linear behavior in the resistivity is observed in the normal state. For $EuFe_{2-x}Co_xAs_2$, the resistivity behaves very differently at T_S and T_N. The in-plane anisotropy starts to emerge even above T_S and increases smoothly through it. As the temperature is lowered further, it takes a dramatic enhancement through the magnetic phase transition. Therefore, our results provide direct evidence ruling out the possibility that the anisotropy is caused by lattice distortion. The dramatic difference of the anisotropies in the

electron- and hole-doped materials suggests that magnetism must be orbital selective in a way that the magnetism in the hole-underdoped iron pnictides may stem mainly from the d_{xy} orbitals while the magnetism in the electron-underdoped ones attributes mainly to the d_{yz} and d_{xz} orbitals.

High quality single crystals with nominal composition $EuFe_{2-x}Co_xAs_2$ ($x = 0, 0.067, 0.1, 0.225$) and $Ba_{1-x}K_xFe_2As_2$ ($x = 0.1, 0.18$) were grown by the self-flux method as described elsewhere [19]. As Co doping increases in $EuFe_{2-x}Co_xAs_2$, the SDW transition and structure transition were gradually separated and suppressed like the $BaFe_{2-x}Co_xAs_2$ system. Resistivity reentrance behavior due to the antiferromagnetic ordering of Eu^{2+} spins is also observed at low temperature. The detailed in-plane resistivity of $EuFe_{2-x}Co_xAs_2$ can be found elsewhere [20,21]. $Ba_{0.9}K_{0.1}Fe_2As_2$ and $Ba_{0.82}K_{0.18}Fe_2As_2$ undergo structural transition and SDW transition at around 128 and 113 K, respectively. It is difficult to directly measure the in-plane resistivity anisotropy because the material naturally forms structure domains below T_S. In order to investigate the intrinsic in-plane resistivity anisotropy we developed a mechanical cantilever device that is able to detwin crystals similar to Ref. [10]. Crystals were cut parallel to the orthorhombic a and b axes so that the orthorhombic a (b) direction is perpendicular (parallel) to the applied pressure direction. The inset of Fig. 1(a) illustrates the diagram of the magnetic structure of the Fe layer below T_N. ρ_a (current parallel to a) and ρ_b (current parallel to b) were measured on the same sample using a standard

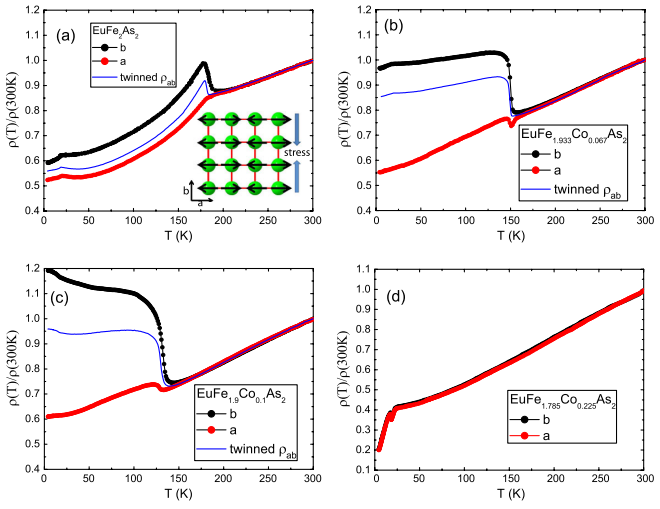

FIG. 1 (color online). Temperature dependence of in-plane resistivity with the electric current flow along a direction (red line) and b direction (black line), respectively, for the parent compound (a) $EuFe_2As_2$, (b) $EuFe_{1.933}Co_{0.067}As_2$, (c) $EuFe_{1.9}Co_{0.1}As_2$, (d) $EuFe_{1.775}Co_{0.225}As_2$. The twinned in-plane resistivity was also shown for comparison (blue line). The inset of (a) shows the diagram of magnetic structure of Fe layer below T_N.

4-point configuration. We have obtained the results similar to those found in Ref. [10] in a Co-doped Ba122 system as shown in Figs. 4(d) and 4(e).

Figure 1(a) shows the temperature dependence of in-plane resistivity with the current flowing parallel to the orthorhombic b direction (black line) and orthorhombic a direction (red line) of the detwinned $EuFe_2As_2$ sample. Compounds with a small amount of Co doping show large in-plane anisotropy as displayed in Figs. 1(b) and 1(c) for $x = 0.067$ and $x = 0.1$, respectively. More specifically, we can find a much more obvious upturn of ρ_b around T_N or T_S compared to the twinned in-plane resistivity as the blue line shows while ρ_a shows no upturn and drops very rapidly with the temperature decreases below T_N or T_S. The behavior of ρ_a is very similar to the $EuFe_2As_2$ polycrystalline samples [22]. When the Co doping increases, the upturn of ρ_b at T_N or T_S becomes much sharper while the drop of ρ_a at T_N or T_S gradually disappears and turns into a small upturn at the temperature slightly lower than ρ_b. For the sample of $x = 0.225$, no in-plane anisotropy was found due to the complete suppression of the structural or magnetic transition as shown in Fig. 1(d). The different behavior of ρ_a and ρ_b observed here is very similar to the ones in other parent or electron-underdoped iron pnictides [10,11].

Further examining our data, we also notice that the structural transition temperature T_S and the magnetic transition temperature T_N become well separated as the Co doping increases in $EuFe_{2-x}Co_xAs_2$. This separation provides us an opportunity to investigate the effects of the structural transition and magnetic transition on the ρ_a and ρ_b separately. The two transition temperatures can be obtained by analyzing the heat capacity of the samples. In order to display the anomalies of heat capacity at the transitions more clearly, we treat the heat capacity in the $x = 0.225$ sample as a background since it does not show phase transition. By subtracting this background, we obtain the electronic part of the heat capacity, ΔC_P, of the $x = 0.067$ and $x = 0.1$ samples as shown in the bottom panels of Figs. 2(a) and 2(b). Taking the $x = 0.067$ sample as an example, the ΔC_P has two distinct features as a function of temperature: a very sharp peak at 150 K and a broad hump around 157 K. Similar to other isostructure materials, such as $BaFe_{2-x}Co_xAs_2$ [23], we can attribute the sharp peak to the SDW transition and the broad hump to the structure transition. In the $x = 0.067$ sample, as shown in Fig. 2(a), ρ_a shows a diplike behavior from T_S to T_N. With decreasing temperature, ρ_a starts to drop rapidly at the temperature coincident with T_S, and after reaching its minimum value, it shows a very weak upturn at the temperature coincident with T_N. ρ_b, however, has no observable feature at T_S but shows a large upturn around T_N. When the sample is not detwinned, the in-plane resistivity ρ_{ab} also shows a large upturn. For the $x = 0.1$ sample, T_S is suppressed to 140 K and T_N is suppressed to 130 K from the heat capacity

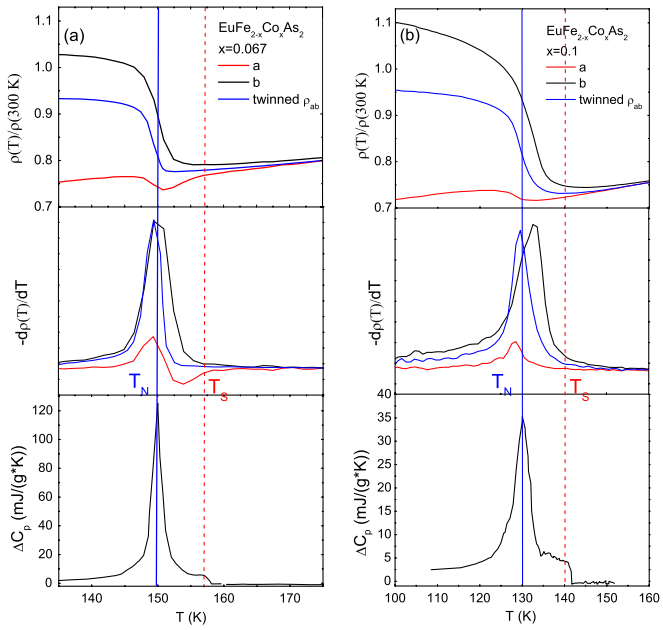

FIG. 2 (color online). Temperature dependence of ρ_a, ρ_b, and twinned ρ_{ab}, their differential curve, and heat capacity around the T_S and T_N for the sample of (a) $x = 0.067$ and (b) $x = 0.1$. The red dashed vertical line and blue solid vertical line indicate T_S and T_N, respectively.

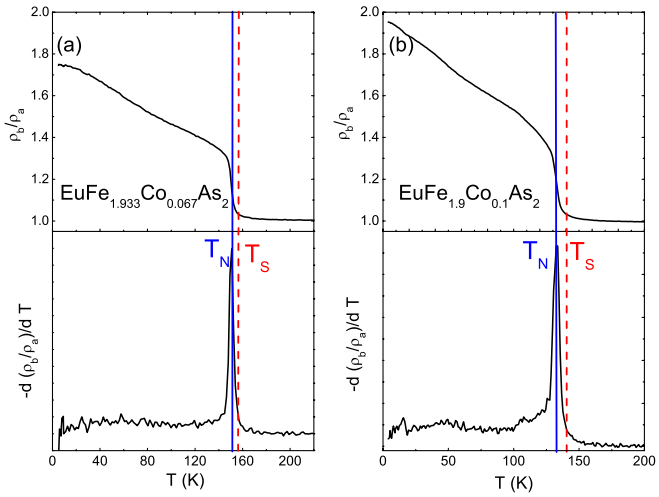

FIG. 3 (color online). In-plane resistivity anisotropy ρ_b/ρ_a and its related differential curve for the sample of (a) $x = 0.067$ and (b) $x = 0.1$. The blue solid vertical line indicates T_N and red dashed vertical line indicates T_S.

measurement as shown in Fig. 2(b). ρ_b starts to go upward above T_S but ρ_a does not show any obvious response. The $d\rho_{ab}/dT$ curve of the twinned ρ_{ab} peaks around T_N while the peak of $d\rho_b/dT$ is higher than T_N and the one of $d\rho_a/dT$ is slightly lower than T_N. With increasing the Co doping, the effect of the structure transition on the ρ_a is gradually wiped out, which is similar to the $BaFe_{2-x}Co_xAs_2$ system, while the upturn behavior T_N becomes more noticeable.

We characterized the degree of in-plane resistivity anisotropy by the ratio ρ_b/ρ_a. Figures 3(a) and 3(b) show in-plane resistivity anisotropy ρ_b/ρ_a and its related differential curve for $x = 0.067$ and $x = 0.1$ samples, respectively. The amplitude of the anisotropy is greatly increased with Co doping though the magnetic transition and structure transition are suppressed, similar to $BaFe_{2-x}Co_xAs_2$. The in-plane resistivity anisotropy increases very rapidly at T_N with decreasing temperature and then gradually increases down to 4 K. A very sharp peak can be observed in the differential curve of ρ_b/ρ_a at the temperature coincident with T_N. However, ρ_b/ρ_a did not show any obvious anomaly at T_S. The sharp increase of in-plane resistivity anisotropy at T_N indicates that in-plane anisotropy is correlated to the magnetic transition rather than structure transition. It also indicates that the in-plane electron anisotropy is driven by the magnetic fluctuation or other hidden electronic order rather than the small orthorhombic distortion.

To understand the common feature of the in-plane resistivity anisotropies in $EuFe_{2-x}Co_xAs_2$ and $BaFe_{2-x}Co_xAs_2$, we plot ρ_a and ρ_b in an enlarged temperature region as shown in Figs. 4(a)–4(e). For $EuFe_{2-x}Co_xAs_2$, it is very clear that the in-plane resistivity anisotropy emerges at temperatures higher than the structure transition temperature as the black arrows indicate. It suggests that fluctuations associated with the resistivity anisotropy must emerge well above the T_S. Moreover, T-linear resistivity behaviors appear in a large temperature region above the temperature at which ρ_a and ρ_b begin to show anisotropy. We also observed this kind of feature in the Co-doped Ba122 system as shown in Figs. 4(d) and 4(e) for $BaFe_2As_2$ and $BaFe_{1.83}Co_{0.17}As_2$, respectively. The T-linear behavior has also been observed in other iron pnictides, for example, $BaFe_2As_{2-x}P_x$ single crystals and $SmO_{1-x}F_xFeAs$ polycrystalline samples [24,25]. Therefore, this behavior might be universal in electron-underdoped iron pnictides at high temperature. The T-linear resistivity behavior is also similar to the one in cuprates. However, in $Ba_{1-x}K_xFe_2As_2$, such a T-linear behavior is rapidly suppressed through K doping. As shown in Figs. 4(f) and 4(g), $Ba_{0.9}K_{0.1}Fe_2As_2$ shows very tiny in-plane anisotropy compared with its parent compound, $Ba_{0.82}K_{0.18}Fe_2As_2$ almost shows no in-plane resistivity anisotropy, and its normal state resistivity does not follow the T-linear behavior.

The different behavior of the in-plane resistivity anisotropy between the hole- and electron-doped materials is a main discovery of our Letter. However, in order to justify that the difference is indeed a difference between their intrinsic electronic properties, we have to show the two materials are both detwinned. The insets of 4(f) are the polarized-light images of the surface for twinned (i) and detwinned (ii) $Ba_{0.9}K_{0.1}Fe_2As_2$ at the temperature of 78 K. The samples are almost fully detwinned as we can no longer see the twin domains.

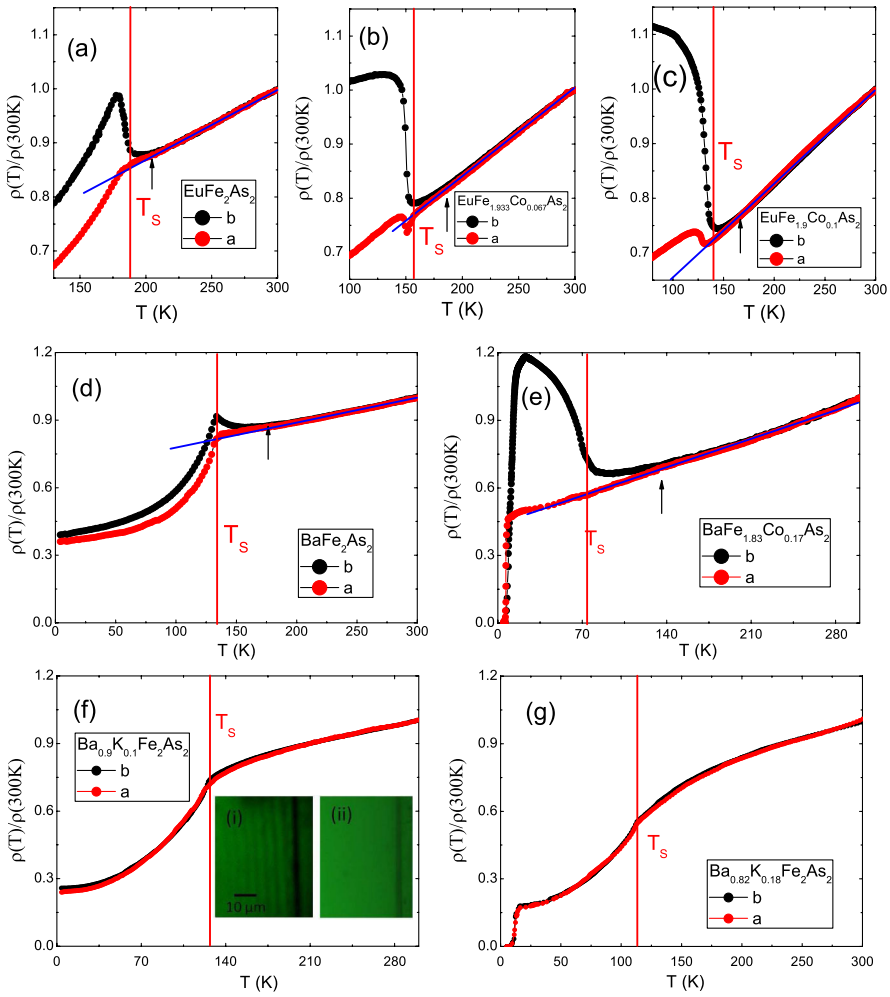

FIG. 4 (color online). The temperature dependence of ρ_a and ρ_b for (a) $EuFe_2As_2$, (b) $EuFe_{1.933}Co_{0.067}As_2$, (c) $EuFe_{1.9}Co_{0.1}As_2$, (d) $BaFe_2As_2$, (e) $BaFe_{1.83}Co_{0.17}As_2$, (f) $Ba_{0.9}K_{0.1}Fe_2As_2$, and (g) $Ba_{0.82}K_{0.18}Fe_2As_2$. The insets of (f) are the polarized-light images of the surface for twinned (i) and detwinned (ii) $Ba_{0.9}K_{0.1}Fe_2As_2$ at the temperature of 78 K. The black arrows indicate the temperature where ρ_a and ρ_b begin to show anisotropy. The red vertical line indicates the T_S. The thin blue line in (a)–(e) is the linear fit of the resistivity above the black arrow indicated temperature.

Our above results have important implications for the origin of the nematicity in iron pnictides. First, our results strongly support the fact that the nematic state in iron pnictides is indeed an electronic nematic state. Our measurements show that the in-plane resistivity anisotropy is closely related to the magnetic transition rather than the structural transition and persists at temperatures higher than structural transition, suggesting the existence of nematicity even in the tetragonal lattice structure, consistent with earlier results in Ref. [10]. Second, the distinct anisotropy of resistivity between the hole- and electron-underdoped materials reveals the hidden interplay between magnetic and orbital degrees of freedom. Many different theories and calculations have been done for the magnetically ordered state [26–33]. Recently, some theories have focused on ferro-orbital order which has an unequal number of electron occupation in the d_{xz} and d_{yz} orbitals [31]. This orbital order breaks the rotational symmetry and causes the lattice distortion [32,33]. Angle-resolved photoemission spectroscopy (ARPES) measurements have provided evidence for such an orbital order [13]. Since there is little anisotropy in the magnetically ordered states of the hole-doped samples, our results suggest that the resistivity anisotropy is most likely induced by orbital order rather than magnetic order. The orbital order is suppressed rapidly by hole doping while it is relatively robust to electron doping. The strong enhancement of the anisotropy around T_N in electron-doped systems indicates that the magnetic ordering and orbital ordering are intimately connected to each other in these systems. However, our result on hole-doped samples suggest that magnetic ordering is not simply a result of orbital ordering. Considering the fact that the dominating orbitals are t_{2g} and the orbital ordering is most likely due to the d_{xz} and d_{yz}, we can conclude that although the magnetically ordered states in both electron- and hole-doped materials have an identical

ordering wave vector, the two states must differ microscopically from their orbital involvements; namely, the magnetism is orbital selective in a way that the magnetic ordering in hole-doped systems is attributed mostly to the d_{xy} orbital while the d_{yz} and d_{xz} make important contributions to the magnetism in the electron doped ones. This implication can be tested explicitly by ARPES experiments in hole-doped materials. Finally, the correspondence between the anisotropy and T-linear behavior suggests the importance of electron-electron correlation in causing the orbital and magnetic ordering. The T-linear resistivity can be understood by the presence of strong orbital or magnetic fluctuations in all three t_{2g} orbitals. Consequently, the suppression of T-linear resistivity behavior by hole doping indicates the suppression of orbital and magnetic fluctuations in the d_{xz} and d_{yz} ones.

In conclusion, we have measured the in-plane resistivity anisotropy on electron-underdoped $EuFe_{2-x}Co_xAs_2$ and $BaFe_{2-x}Co_xAs_2$ and hole-underdoped $Ba_{1-x}K_xFe_2As_2$ single crystals. Large in-plane resistivity anisotropy was found in $EuFe_{2-x}Co_xAs_2$, which is quite similar to the isostructural $BaFe_{2-x}Co_xAs_2$ system; however, anisotropy disappears in hole-doped samples. A correspondence between the anisotropy and a T-linear behavior of resistivity at high temperature is found to be present universally in all samples measured so far. The different behavior of the anisotropy at T_N and T_S rules out the possibility that the anisotropy originates from the lattice degree of freedom. The magnetic states in the hole- and electron-doped systems are significantly different.

This work is supported by the National Natural Science Foundation of China (973 Program No. 2011CB00101 and Grant No. 51021091), the Ministry of Science and Technology of China, and Chinese Academy of Sciences.

*Corresponding author.
chenxh@ustc.edu.cn

[1] Y. Kamihara *et al.*, J. Am. Chem. Soc. **130**, 3296 (2008).
[2] X. H. Chen *et al.*, Nature (London) **453**, 761 (2008).
[3] Z. A. Ren *et al.*, Europhys. Lett. **83**, 17002 (2008).
[4] M. Rotter, M. Tegel, and D. Johrendt, Phys. Rev. Lett. **101**, 107006 (2008).
[5] C. Fang *et al.*, Phys. Rev. B **77**, 224509 (2008).
[6] C. Xu, M. Muller, and S. Sachdev, Phys. Rev. B **78**, 020501 (2008).
[7] F. Krüger *et al.*, Phys. Rev. B **79**, 054504 (2009).
[8] C. C. Lee, W. G. Yin, and W. Ku, Phys. Rev. Lett. **103**, 267001 (2009).
[9] B. Valenzuela, E. Bascones, and M. J. Calderon, Phys. Rev. Lett. **105**, 207202 (2010).
[10] Jiun-Haw Chu *et al.*, Science **329**, 824 (2010).
[11] M. A. Tanatar *et al.*, Phys. Rev. B **81**, 184508 (2010).
[12] Jun Zhao *et al.*, Nature Phys. **5**, 555 (2009).
[13] T. Shimojima *et al.*, Phys. Rev. Lett. **104**, 057002 (2010).
[14] T.-M. Chuang *et al.*, Science **327**, 181 (2010).
[15] M. P. Lilly *et al.*, Phys. Rev. Lett. **82**, 394 (1999).
[16] R. A. Borzi *et al.*, Science **315**, 214 (2007).
[17] Y. Ando *et al.*, Phys. Rev. Lett. **88**, 137005 (2002).
[18] V. Hinkov *et al.*, Science **319**, 597 (2008).
[19] X. F. Wang *et al.*, Phys. Rev. Lett. **102**, 117005 (2009).
[20] Y. He *et al.*, J. Phys. Condens. Matter **22**, 235701 (2010).
[21] J. J. Ying *et al.*, Phys. Rev. B **81**, 052503 (2010).
[22] Zhi Ren *et al.*, Phys. Rev. B **78**, 052501 (2008).
[23] Jiun-Haw Chu *et al.*, Phys. Rev. B **79**, 014506 (2009).
[24] S. Kasahara *et al.*, Phys. Rev. B **81**, 184519 (2010).
[25] R. H. Liu *et al.*, Phys. Rev. Lett. **101**, 087001 (2008).
[26] D. J. Singh, Phys. Rev. B **78**, 094511 (2008).
[27] J. W. Lynn *et al.*, Physica (Amsterdam) **469C**, 469 (2009).
[28] W. Lv, J. Wu, and P. Phillips, Phys. Rev. B **80**, 224506 (2009).
[29] S. P. Kou *et al.*, Europhys. Lett. **88**, 17 010 (2009).
[30] M. D. Johannes and I. I. Mazin, Phys. Rev. B **79**, 220510 (R) (2009).
[31] C.-C. Chen *et al.*, Phys. Rev. B **82**, 100504(R) (2010).
[32] W. Lv, F. Kruger, and P. Phillips, Phys. Rev. B **82**, 045125 (2010).
[33] W. G. Yin, C. C. Lee, and W. Ku, Phys. Rev. Lett. **105**, 107004 (2010).